

## Low-temperature structures of Xe on graphite in the one- to two-layer regime

Hawoong Hong and R. J. Birgeneau

*Department of Physics, Massachusetts Institute of Technology, Cambridge, Massachusetts 02139*

M. Sutton

*Department of Physics, McGill University, Montreal, Quebec, Canada H3A 2T8*

(Received 24 July 1985)

We have investigated the low-temperature structures of xenon overlayers on graphite with coverages ranging from 0.8 to 1.7 ( $\sqrt{3} \times \sqrt{3}$ ) monolayers. We find that below 60 K the full monolayer has an incommensurate structure which appears to correspond to a rectangular striped phase rather than the  $\sqrt{3} \times \sqrt{3}$  commensurate structure inferred from previous electron-diffraction studies. With increasing coverage there is a first-order transition from the monolayer striped phase to a bilayer hexagonal structure close to that of bulk xenon.

### I. INTRODUCTION

The physics of rare gases physisorbed onto the basal planes of graphite continues to be the subject of extensive investigation.<sup>1-9</sup> Much work has centered on the nature of melting in the monolayer coverage region.<sup>5-9</sup> A variety of novel effects also occurs due to the competition between the adsorbate-adsorbate potential and the adsorbate-substrate interaction. Both the structures that result and the transitions between them often involve quite subtle features which are a challenge to modern theories of two-dimensional (2D) matter.<sup>10</sup> Equally interesting issues arise in the nature of the evolution from thin to thick overlayers.<sup>11,12</sup> So far, there is a paucity of accurate structural data for the evolution from monolayer to bilayer to trilayer coverages, etc. Such information is essential for understanding solid-state wetting.

In this paper we describe a set of x-ray scattering measurements on xenon on graphite at low temperatures in the monolayer and bilayer coverage regimes. The melting transitions at high temperatures for monolayer xenon have been extensively investigated with x rays.<sup>7,8</sup> However, there are only limited x-ray data at low temperatures.<sup>13</sup> Monolayer xenon on graphite for  $T < 80$  K has been studied by Schabes-Retchkiman and Venables<sup>14</sup> using transmission high-energy electron diffraction (THEED). These authors suggest that a hexagonal incommensurate to hexagonal ( $\sqrt{3} \times \sqrt{3}$ ) $R 30^\circ$  commensurate transition occurs with decreasing temperature at  $\sim 65$  K. As we shall discuss, our data strongly suggest instead an hexagonal incommensurate to stripe domain transition at  $\sim 65$  K for coverages near one monolayer. With increasing coverage for  $T < 65$  K there is a first-order transition from the monolayer stripe structure to a bilayer hexagonal structure. We note that the existence of the monolayer stripe structures at low temperature was predicted by Bak *et al.*<sup>15</sup> a number of years ago but, because of either resolution or equilibrium difficulties, has only now been seen.

### II. EXPERIMENTAL TECHNIQUE

The experimental techniques utilized in these experiments are standard ones in our laboratory and have been

extensively discussed previously.<sup>3,7,12</sup> The measurements utilized a triple-axis x-ray spectrometer with Cu  $K_\alpha$  radiation from a Rigaku 12-kW rotating anode source operating at 8 kW. For most of the experiments we used a vertically bent LiF (200) monochromator and flat LiF (200) analyzer. The consequent longitudinal resolution was  $0.0033 \text{ \AA}^{-1}$  half-width at half-maximum (HWHM). The one-to two-layer measurements utilized a bent graphite monochromator and Soller slits before the detector; in these latter experiments the resolution was  $0.01 \text{ \AA}^{-1}$  HWHM. The substrate used was Union Carbide vermicular graphite from the same batch as that utilized by Mochrie *et al.*<sup>12</sup> This has no preferred orientation, a large specific area, and a surface coherence length of 500 Å. The consequent finite-size broadening of the diffraction profiles is  $0.006 \text{ \AA}^{-1}$  HWHM, that is, approximately twice the resolution of the LiF spectrometer configuration. Vermicular graphite is preferable to Union Carbide ZYX for multilayer studies because of its limited alternate site adsorption and superior equilibrium properties at low temperatures.<sup>3</sup>

The data were fitted using the techniques discussed extensively by Stephens *et al.*<sup>3</sup> The commensurate krypton profile was fitted to the Gaussian plus Lorentzian form [Eq. (5) of Ref. 3], while all incommensurate peaks were fitted to a resolution-limited powder-averaged Lorentzian convoluted with the resolution and finite-size functions. We note that Heiney *et al.*<sup>7</sup> have demonstrated that the power-law line shape expected for a floating solid is well represented by a sharp powder-averaged Lorentzian convoluted with the instrumental resolution function. The latter is much more convenient computationally.

### III. EXPERIMENTAL RESULTS

The measured profile for commensurate Kr on graphite is shown in Fig. 1 for coverage ( $f$ ) of  $f = 0.89$  and a temperature  $T = 83.8$  K. In this paper all coverages are measured in units of the  $\sqrt{3} \times \sqrt{3}$  structure with full coverage being  $f = 1$ . The solid line in Fig. 1 is the Stephen's commensurate line shape<sup>3</sup> with the finite size and resolution width fixed as above for the LiF spectrometer configuration. The peak position taken as  $Q_{\text{comm}} = 1.701 \text{ \AA}^{-1}$  is

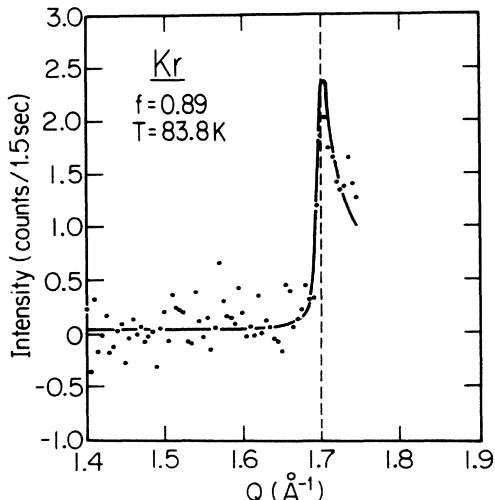


FIG. 1. Diffraction profile of commensurate Kr on graphite with the LiF spectrometer configuration; the graphite background has been subtracted. The solid line is a model commensurate line shape as discussed in the text.

determined directly from the graphite. The graphite background with no krypton in the cell has been subtracted. Thus the only adjustable line-shape parameter is the overall intensity. A slight adjustment in the background has been made to optimize the fit. Although the statistics are poor it is evident that the measured krypton commensurate profile is well described by the model line shape with the predetermined particle size of 500 Å.

We carried out similar measurements as a function of temperature for xenon with several coverages in the neighborhood of  $f=1$ . We discuss first the data for  $f=0.8$ . This coverage, which is in the gas-solid coexistence region below the 2D triple point of 99 K, has been previously studied by Hammonds and co-workers<sup>13</sup> and our results agree with theirs. Representative diffraction profiles at  $T=61.0$  and 25.1 K are shown in Fig. 2. The solid lines correspond to single, resolution-limited Lorentzian profiles; it is evident that the fits are very good and specifically the HWHM of the leading edges are identical within the errors to that of the commensurate Kr scan shown in Fig. 1. The solid lines include the effects of the interfer-

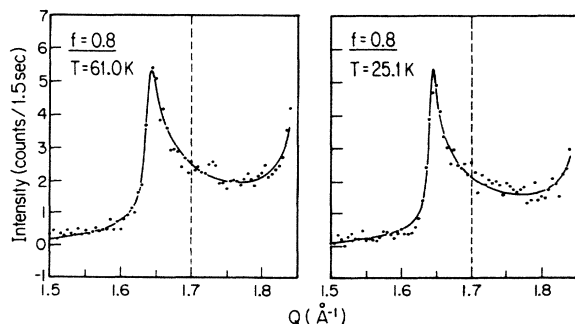


FIG. 2. Diffraction profiles at two temperatures of a Xe layer of coverage 0.8 using the LiF spectrometer configuration. The solid lines are best fits to powder-averaged 2D Lorentzians as discussed in the text.

ence between the Xe overlayer and the graphite on the graphite (0,0,2) reflection centered at  $1.878 \text{ \AA}^{-1}$ ; here we used the formula of Rayment *et al.*<sup>16</sup> The fitted distance between the graphite and xenon layers is  $3.35 \pm 0.1 \text{ \AA}$  compared to the Lennard-Jones value of 3.34 Å. In agreement with Hammonds,<sup>13</sup> we conclude that the low-temperature solid at "monolayer" gas-solid coexistence has an incommensurate hexagonal structure.

The behavior for  $f=0.9$  is quite different. A series of (1,0) diffraction profiles for  $f=0.9$  is shown in Fig. 3. The scan for  $f=0.9$ ,  $T=88.2 \text{ K}$  is essentially identical to those shown in Fig. 2 for  $f=0.8$ , and specifically the HWHM of the leading edge is determined by the graphite particle size convoluted with the instrumental resolution. There is also the suggestion of a weak peak at  $\sim 1.72 \text{ \AA}^{-1}$ . The solid line for  $f=0.9$ ,  $T=88.2 \text{ K}$  is the result of a fit to a Lorentzian profile centered at  $Q_{\text{comm}} - \epsilon$  together with a weak peak at  $Q_{\text{comm}} + \epsilon/2$ . The fitted inverse correlation length is  $\kappa=0.003 \text{ \AA}^{-1}$ , much less than the finite-size width of  $0.006 \text{ \AA}^{-1}$ . As noted previously, power-law singularities at a given resolution are well represented by a Lorentzian with width much less than the resolution. The feature at  $+\epsilon/2$  is probably a modulation peak due to the interaction with the substrate.<sup>3</sup>

Based on the THEED results,<sup>14</sup> we expected to observe an incommensurate-commensurate transition with decreasing temperature at  $\sim 65 \text{ K}$ . Comparison of the data in Fig. 3 with the Kr profile in Fig. 1 shows that the xe-

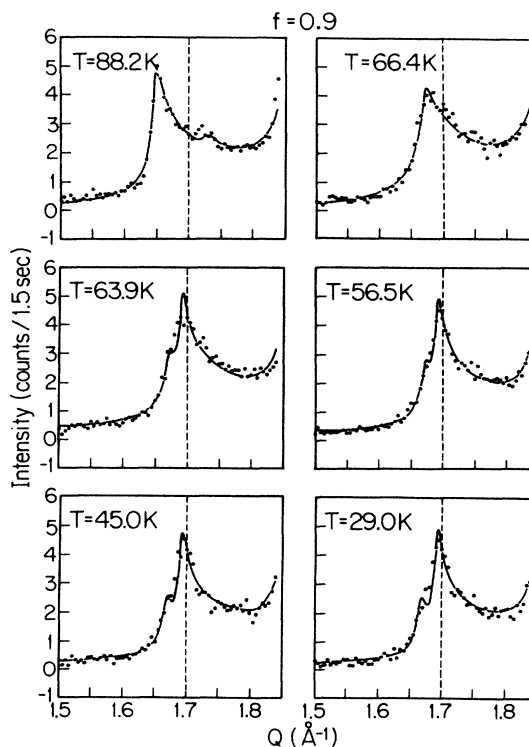


FIG. 3. Diffraction profiles of a Xe  $f=0.9$  submonolayer with the LiF x-ray configuration; the solid lines for  $T=88.2$  and 66.4 K are resolution-limited powder-averaged Lorentzians as discussed in the text; for  $T \leq 63.9 \text{ K}$  the lines are resolution-limited powder-averaged Lorentzians centered at  $Q_{\text{comm}} - \epsilon/4$  and  $Q_{\text{comm}} - \epsilon$  with relative intensity 2:1.

non overlayer is always incommensurate, albeit subtly so. Further, in contrast with the behavior for  $f=0.8$  the HWHM of the leading edge approximately doubles below  $\sim 70$  K; identical behavior for the width was found with THEED.<sup>14</sup> Initially, we fitted the low-temperature profiles with a single Lorentzian peak. A representative fit at 56.5 K is shown in Fig. 4; this requires a net width significantly broader than that determined by the finite particle size. Further, in all of the fits there is a systematic sigmoidal deviation from the model shape on the leading edge. Indeed, many of the scans below 65 K seem to indicate that the leading edge is structured. The poor counting statistics preclude a definitive statement for any single scan, but cumulatively all of the profiles below 65 K, including a number not shown, are consistent with a two-component leading edge.

Accordingly, we then tried fits to a two-peak structure. We first assumed a mixture of commensurate and incommensurate phases. A representative fit to this model is shown on the right-hand side of Fig. 4. It is evident that this model is unsatisfactory. As we noted in the Introduction, several years ago Bak *et al.*<sup>15</sup> predicted that for nearly-commensurate 2D overlayers on graphite at low temperatures the hexagonal symmetry should be broken and a rectangular stripe domain phase should be established provided, as seems physically reasonable, that the domain-wall crossing energy is positive. We therefore analyzed the 0.9 coverage data using this model.

For a simple uniaxial expansion from a commensurate structure in the  $(100)_{\text{Gr}}$  direction, the sixfold degeneracy of the  $(1,0)$  peak is broken and one has two peaks with  $|Q| = Q_{\text{comm}} - \epsilon$  and four peaks with  $|Q| = Q_{\text{comm}} - \epsilon/4$  (see Ref. 3, Fig. 16). Thus, in a powder pattern one expects peaks at  $Q_{\text{comm}} - \epsilon$  and  $Q_{\text{comm}} - \epsilon/4$  with an intensity ratio 1 to 2. The solid lines in Fig. 3 for  $T \leq 63.9$  K are calculated using this model. The inverse correlation lengths  $\kappa$  in the Lorentzian are of the same order as the value determined from the 88.2-K profile and much less than the resolution width. The fitted incommensurability is  $\epsilon = 0.03 \text{ \AA}^{-1}$  for  $T \leq 60$  K. It is evident that the model describes the measured profiles quite well. Similar agreement is found for other temperatures and coverages. In the next section we shall examine the

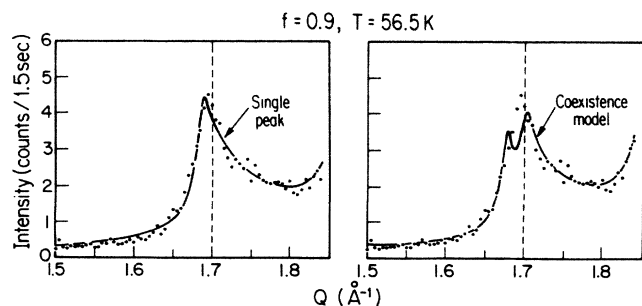


FIG. 4. Model fits to the diffraction profiles for a coverage of 0.9 Xe layers at 56.5 K; the left-hand side is a single broadened Lorentzian, the right-hand side is two resolution-limited peaks, one fixed at  $Q_{\text{comm}}$ .

domain-wall structure and thence justify the uniform rectangular expansion approximation for the fits. We should note that the profiles for  $T \leq 63.9$  K are slightly broader than resolution. We assume that this reflects effects of domain-wall pinning due to impurities and the boundaries.

We now discuss the evolution of the structure from the monolayer to the bilayer regime. Data for  $f=0.8$  and 0.9 with LiF resolution are shown in Figs. 2 and 3. We also carried out a series of measurements for coverages varying from  $f=1.02$  to 1.72 using the lower resolution Gr monochromator spectrometer configuration. A typical set of scans at  $T \sim 59$  K is shown in Fig. 5. The solid line for  $f=1.02$  is calculated using the stripe domain model with  $\kappa=0.002 \text{ \AA}^{-1}$  and  $\epsilon=0.02 \text{ \AA}^{-1}$ ; because of the poorer resolution the two-component structure of the peak is not evident. Nevertheless, other models all fit the data less well and specifically neither hexagonal commensurate nor hexagonal incommensurate line shapes are acceptable. The solid line for  $f=1.72$  is calculated assuming an ideal bilayer hexagonal incommensurate structure with  $AB$  stacking; the width of the leading edge is determined by the 500-Å particle size and the instrumental resolution; for  $f=1.72$  and  $Q_0=1.66 \text{ \AA}^{-1}$  the density is  $\sim 90\%$  of the full value assuming complete coverage of the substrate. The solid lines for  $f=1.36$  and 1.57 are calculated assuming two-phase coexistence between the  $f=1.02$  and 1.72 structures with a law-of-levers rule for the relative intensities. Given that there are no adjustable parameters, the model profiles describe the data quite well. This provides strong evidence that at  $T \sim 59$  K, and presumably at lower temperatures, there is a first-order transition between a monolayer stripe domain structure and a bilayer hexagonal structure. The bilayer lattice constant agrees within 0.3% with that of bulk xenon at the same temperature.<sup>17</sup> More-detailed measurements as a function of cov-

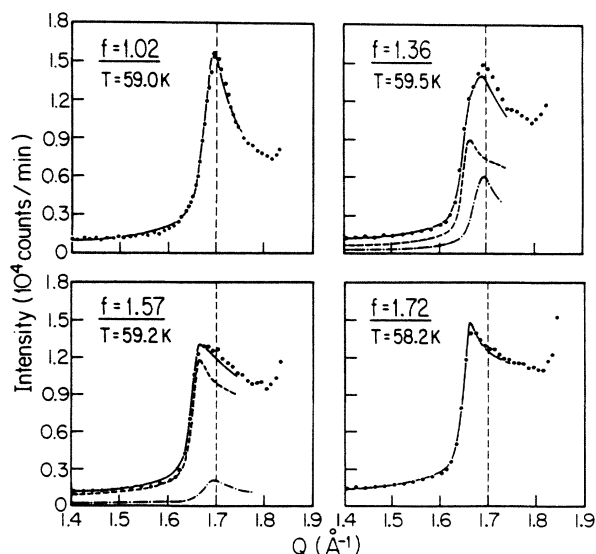


FIG. 5. Diffraction profiles of Xe layers using the graphite lineup; the solid lines are discussed in the text.

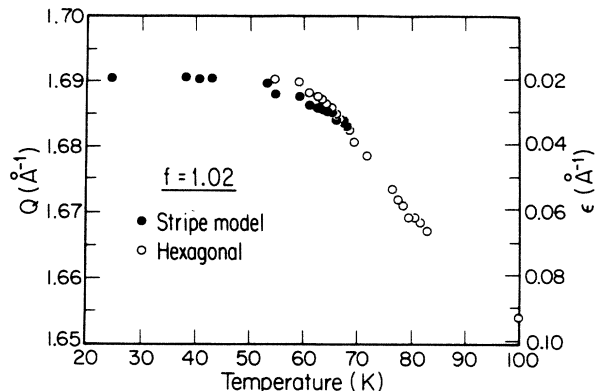


FIG. 6. Fitted peak position ( $Q$ ) and peak displacement ( $\epsilon$ ) from commensurate peak position.  $\circ$ 's are the  $Q$  of the incommensurate solid.  $\bullet$ 's are the  $\epsilon$ 's of the stripe phase.

erage will be required to establish the monolayer and bilayer boundaries precisely. We consider it to be an important and surprising result that already at two layers the xenon film structure is close to that of the bulk,<sup>13,14</sup> while the monolayer structure is controlled by the substrate.

In Fig. 6 we show the  $(1,0)$  wave vector as a function of temperature for  $f = 1.02$ . For the stripe model we have plotted  $Q_{\text{comm}} - \epsilon/2$  which is the weighted mean  $Q$  vector. We cannot distinguish between the stripe and hexagonal models between  $\sim 70$  and  $60$  K. High-resolution synchrotron x-ray studies, ideally on a single crystal, are required to elucidate the detailed nature of the incommensurate hexagonal-stripe transition and, indeed, to confirm our identification of the low-temperature structure as the stripe phase of Bak *et al.*<sup>15</sup> Interesting rotational effects may also occur.

Finally, for completeness we show in Fig. 7 a fit to the  $f = 1.02$  scan at  $62.6$  K including the Gr  $(0,0,2)$  interference region. This illustrates that the formula of Rayment *et al.*<sup>16</sup> works extremely well in the monolayer coverage region. Our fits to the bilayer interference effects were somewhat less successful; the latter requires further research.

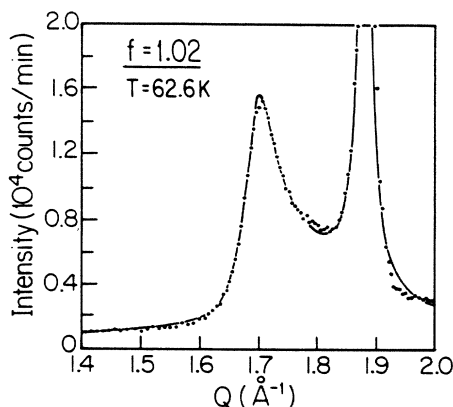


FIG. 7. Fit to the  $f = 1.02$ ,  $T = 62.6$  K Xe profile including the Gr  $(0,0,2)$  interference region.

#### IV. DISCUSSION

As reported in the preceding section, the profiles for  $f = 0.9$  and  $1.02$  are consistent with a structure in which the xenon is commensurate in the  $(\bar{1}20)_{\text{Gr}}$  direction and uniformly expanded in the  $(100)_{\text{Gr}}$  direction. It is of interest to relate this to the corresponding domain-wall model. As discussed by Kardar and Berker,<sup>2</sup> for a uniaxial expansion one may have either superlight or light walls; these are illustrated in Figs. 8 and 9, respectively. In order to determine the actual domain-wall structure we carried out a simple  $T = 0$  classical computer simulation. We first established a uniform structure with the boundary atoms fixed at the positions shown in Figs. 8 and 9 in order to preserve the overall phase shift, and we assumed periodic boundary conditions. We then gradually turned on the substrate potential and moved the atoms simultaneously to minimize the potential energy. We terminated with the potentials given by Steele,<sup>18</sup> the final configurations are shown in Figs. 7 and 8. We note that the wall widths are 4 or 5 atomic spacings; similar values have been found for hexagonal incommensurate Kr on graphite.<sup>19</sup> We note that increasing the substrate modulation potential to the value given by Vidali and Cole<sup>18</sup> does not change these results qualitatively.

The resultant diffraction profiles are shown in Fig. 10. It is evident that only the relaxed superlight wall model agrees with experiment. Concomitantly, the walls are sufficiently broad relative to their mean spacing (32 rows of xenon atoms in our model calculation) that the diffraction profile is barely distinguishable from that of the uniform expansion model. This justifies the analysis used in the preceding section. A single-crystal diffraction study to search for the predicted superlattice peaks would clearly be invaluable.

We conclude with several observations. We believe that our data are consistent with the THEED results,<sup>14</sup> but our more accurate  $Q$ -resolution and line-shape analysis has allowed us to distinguish between a weakly incommensurate stripe domain structure and a hexagonal commensurate structure. Schabes-Retchkiman and Venables<sup>14</sup> have criticized the power-law analysis used for the monolayer Kr

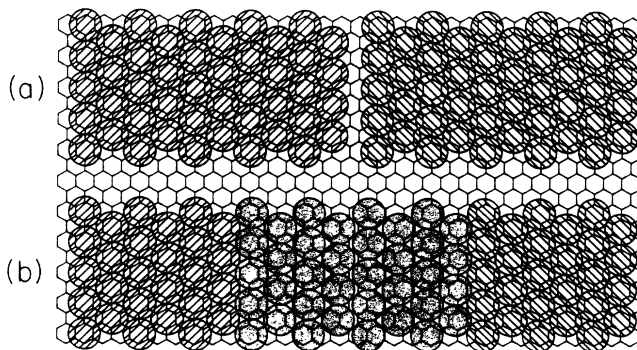


FIG. 8. (a) Sharp superlight domain wall. (b) Relaxed superlight domain wall. Shaded circles indicate atoms whose positions deviate significantly from the commensurate position.

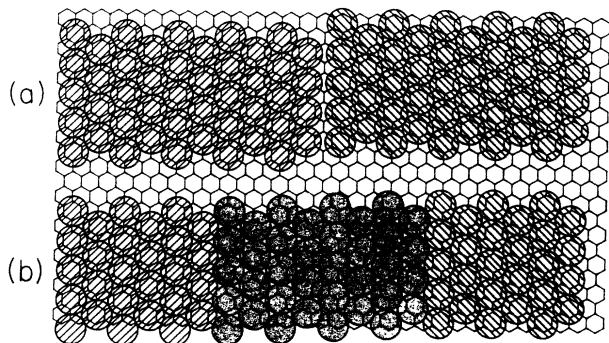


FIG. 9. (a) Sharp light domain wall. (b) Relaxed light domain wall. Shaded circles indicate atoms whose positions deviate significantly from the commensurate position.

graphite commensurate-incommensurate transition<sup>3,20</sup> on the basis that universality would necessitate that Xe behave similarly. Clearly, their criticism is no longer relevant. In the analysis of Bak *et al.*,<sup>15</sup> the stripe domain structure is preferred over a hexagonal structure because of the assumed positive wall crossing energy. At higher temperatures entropy favors the hexagonal structure.<sup>21</sup> This picture is clearly consistent with our data. Halpin-Healy and Kardar<sup>10</sup> have carried out a detailed theory of the Kr system and have predicted that below  $\sim 47$  K a striped structure should intervene between the hexagonal commensurate and incommensurate phases. For Kr the stripe domain phase has not yet been observed. We hope that these experiments will inspire similar calculations for Xe on graphite. More precise experiments to map out the detailed location of the phase boundaries would also be invaluable.

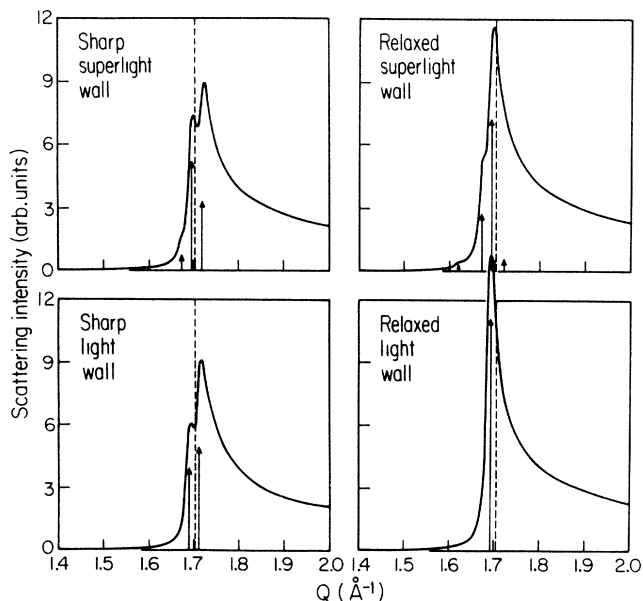


FIG. 10. Powder-averaged patterns for the domain-wall structures shown in Figs. 7 and 8. Each arrow indicates the relative scattering intensity at the corresponding  $Q$ ; the calculated profiles use the resolution parameters for the LiF spectrometer configuration.

#### ACKNOWLEDGMENTS

We are grateful to P. M. Horn, S. G. J. Mochrie, E. Specht, and P. W. Stephens for stimulating discussions about this work. The work at Massachusetts Institute of Technology was supported by the United States Army Research Office (Durham, NC) under Contract No. DAAG29-85-K-0058.

- <sup>1</sup>See, for example, papers in *Ordering in Two Dimensions*, edited by S. K. Sinha (Elsevier, New York, 1980).
- <sup>2</sup>M. Kardar and A. N. Berker, *Phys. Rev. Lett.* **48**, 1552 (1982).
- <sup>3</sup>P. W. Stephens, P. A. Heiney, R. J. Birgeneau, P. M. Horn, D. E. Moncton, and G. S. Brown, *Phys. Rev. B* **29**, 3512 (1984). See also, R. J. Birgeneau, P. A. Heiney, and J. P. Pelz, *Physica* **109-110B**, 1785 (1982).
- <sup>4</sup>F. F. Abraham, W. E. Ridge, D. J. Auerbach, and S. W. Koch, *Phys. Rev. Lett.* **52**, 445 (1984).
- <sup>5</sup>J. P. McTague, J. Als-Nielsen, J. Bohr, and M. Nielsen, *Phys. Rev. B* **25**, 7765 (1982).
- <sup>6</sup>A. D. Migone, A. R. Li, and M. H. W. Chan, *Phys. Rev. Lett.* **53**, 810 (1984).
- <sup>7</sup>P. A. Heiney, P. W. Stephens, R. J. Birgeneau, P. M. Horn, and D. E. Moncton, *Phys. Rev. B* **28**, 6416 (1983).
- <sup>8</sup>E. D. Specht, R. J. Birgeneau, K. L. D'Amico, D. E. Moncton, S. E. Nagler, and P. M. Horn, *J. Phys. (Paris) Lett.* **46**, L561 (1985), and references therein.
- <sup>9</sup>S. B. Hurlbut and J. G. Dash, *Phys. Rev. Lett.* **53**, 1931 (1985).
- <sup>10</sup>R. G. Caflisch, A. N. Berker, and M. Kardar, *Phys. Rev. B* **31**, 4527 (1985), and references therein; T. Halpin-Healy and M. Kardar, *ibid.* **31**, 1664 (1985).
- <sup>11</sup>J. G. Dash, *Phys. Rev. B* **15**, 3136 (1977); R. Pandit, M. Schick, and M. Wortis, *ibid.* **26**, 5112 (1982).
- <sup>12</sup>S. G. J. Mochrie, M. Sutton, R. J. Birgeneau, D. E. Moncton,

- and P. M. Horn, *Phys. Rev. B* **30**, 263 (1984).
- <sup>13</sup>E. M. Hammonds, P. A. Heiney, P. W. Stephens, R. J. Birgeneau, and P. M. Horn, *J. Phys. C* **13**, L301 (1980); E. M. Hammonds, M. Sc. thesis, Massachusetts Institute of Technology, 1980; R. J. Birgeneau, E. M. Hammonds, P. A. Heiney, P. W. Stephens, and P. M. Horn, Ref. 1, pp. 29–38.
- <sup>14</sup>P. S. Schabes-Retchkiman and J. A. Venables, *Surf. Sci.* **105**, 536 (1981).
- <sup>15</sup>P. Bak, D. Mukamel, J. Villain, and K. Wentowska, *Phys. Rev. B* **19**, 1610 (1979).
- <sup>16</sup>T. Rayment, R. K. Thomas, G. Bomchil, and J. White, *Mol. Phys.* **433**, 601 (1981).
- <sup>17</sup>G. H. Cheesman and C. M. Soane, *Proc. Phys. Soc. London, Sect. B* **70**, 700 (1957).
- <sup>18</sup>W. A. Steele, *Surf. Sci.* **36**, 317 (1973); see also, G. Vidali and M. W. Cole, *Phys. Rev. B* **29**, 6736 (1984).
- <sup>19</sup>K. L. D'Amico, D. E. Moncton, E. D. Specht, R. J. Birgeneau, S. E. Nagler, and P. M. Horn, *Phys. Rev. Lett.* **53**, 2250 (1984), and references therein.
- <sup>20</sup>S. C. Fain, Jr., M. D. Chinn, and R. D. Diehl, *Phys. Rev. B* **21**, 4170 (1980).
- <sup>21</sup>J. Villain, in *Ordering in Strongly Fluctuating Condensed Matter Systems*, edited by T. Riste (Plenum, New York, 1980).

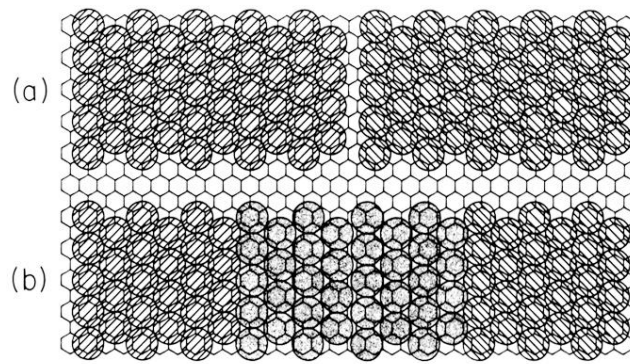


**FIG. 8.** (a) Sharp superlight domain wall. (b) Relaxed superlight domain wall. Shaded circles indicate atoms whose positions deviate significantly from the commensurate position.

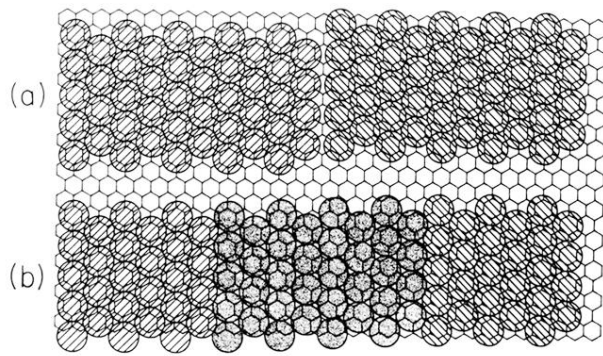


FIG. 9. (a) Sharp light domain wall. (b) Relaxed light domain wall. Shaded circles indicate atoms whose positions deviate significantly from the commensurate position.